

Placement of Deep Brain Electrodes in the Dog Using the Brainsight Frameless Stereotactic System: A Pilot Feasibility Study

S. Long, S. Frey, D.R. Freestone, M. LeChevoir, P. Stypulkowski, J. Giftakis, and M. Cook

Background: Deep brain stimulation (DBS) together with concurrent EEG recording has shown promise in the treatment of epilepsy. A novel device is capable of combining these 2 functions and may prove valuable in the treatment of epilepsy in dogs. However, stereotactic implantation of electrodes in dogs has not yet been evaluated.

Objective: To evaluate the feasibility and safety of implanting stimulating and recording electrodes in the brain of normal dogs using the Brainsight system and to evaluate the function of a novel DBS and recording device.

Animals: Four male intact Greyhounds, confirmed to be normal by clinical and neurologic examinations and hematology and biochemistry testing.

Methods: MRI imaging of the brain was performed after attachment of fiducial markers. MRI scans were used to calculate trajectories for electrode placement in the thalamus and hippocampus, which was performed via burr hole craniotomy. Postoperative CT scanning was performed to evaluate electrode location and accuracy of placement was calculated. Serial neurologic examinations were performed to evaluate neurologic deficits and EEG recordings obtained to evaluate the effects of stimulation.

Results: Electrodes were successfully placed in 3 of 4 dogs with a mean accuracy of 4.6 ± 1.5 mm. EEG recordings showed evoked potentials in response to stimulation with a circadian variation in time-to-maximal amplitude. No neurologic deficits were seen in any dog.

Conclusions and Clinical Importance: Stereotactic placement of electrodes is safe and feasible in the dog. The development of a novel device capable of providing simultaneous neurostimulation and EEG recording potentially represents a major advance in the treatment of epilepsy.

Key words: Canine; Deep brain stimulation; Electroencephalography; Epilepsy.

Epilepsy in the dog is a common and frequently debilitating condition that often leads to a shortened lifespan, death, and major distress for owners of affected dogs.^{1–4} The disease in dogs occurs at a frequency similar to epilepsy in people, with seizures occurring in 0.5–5% of all dogs and with idiopathic epilepsy being the most common underlying cause.^{5,6} Although antiepileptic drugs (AEDs) continue to form the cornerstone of epilepsy treatment in this species, up to 25% of epileptic dogs remain refractory to medication.⁶ This compares to a similar proportion in the human epileptic population, among whom approximately one third continue to suffer seizures despite medication.⁷ For a subset of human patients with hippocampal sclerosis, resection of the mesial temporal lobe will result in a reduction in seizure frequency of 80–90%, but for many patients this is inappropriate because of the location of the seizure focus, unacceptable adverse effects such as memory impairment, or

Abbreviations:

ANT	anterior nucleus of the thalamus
CMT	centromedian nucleus of the thalamus
DBS	deep brain stimulation
EEG	electroencephalogram
EP	evoked potential
MRI	magnetic resonance imaging

multiple seizure types.⁸ As a result, other potential treatments are actively being investigated.^{9,10}

The success of vagal nerve stimulation as a form of neurostimulation capable of improving seizure control has led to research into deep brain stimulation (DBS) as a treatment for epilepsy in recent years.^{9,11–20} Targets proposed for stimulation have included the anterior nucleus of the thalamus (ANT), the centromedian nucleus of the thalamus (CMT), the subthalamic nucleus, and the hippocampus.²¹ Much of this work has been performed in rodent models and has provided valuable insight into the pathogenesis of seizures. However, rodent models suffer from disadvantages related to their size and dissimilar anatomy as compared with people. For this reason, large animal models such as the sheep and minipig are being developed that will allow better translation of DBS strategies into people. Recently, one such study has investigated the feasibility of implanting leads into the ANT and hippocampus of a sheep model as part of the evaluation of a novel device capable of both stimulating and recording from the brain.^{22,23}

Vagal nerve stimulation as a treatment for epilepsy in dogs has shown some promise, suggesting that

Section of Neurology and Neurosurgery, Faculty of Veterinary Science, University of Melbourne, Melbourne, Australia (Long, LeChevoir); Rogue Research Inc, Montreal, Canada (Frey); Department of Medicine, University of Melbourne, St Vincent's Hospital, Melbourne, Australia (Freestone, Cook); and Medtronic Inc, Minneapolis, MN (Stypulkowski, Giftakis).

Corresponding author: S. Long, Senior Lecturer and Head of Neurology and Neurosurgery, University of Melbourne Veterinary Hospital, 250 Princes Hwy, Werribee, Victoria 3030, Australia; email: snlong@unimelb.edu.au

Submitted July 16, 2013; Revised September 3, 2013; Accepted September 19, 2013.

Copyright © 2013 by the American College of Veterinary Internal Medicine

10.1111/jvim.12235

electrical stimulation of the nervous system in this species also may be capable of improving seizure control.²⁴ With the advent of the Brainsight system and other frameless stereotaxy devices, it has recently become possible to access deep regions of the brain in dogs and potentially to stereotactically implant DBS electrodes.^{25,26} Given the potential for epileptic dogs to provide a spontaneous model in which to test thalamic stimulation, therefore, the aim of this study was to investigate the feasibility and safety of placement of stimulating and recording electrodes in the ANT and hippocampus of normal dogs using the Brainsight system, as well as to test a novel device capable of providing DBS in conjunction with simultaneous EEG recording.

Materials and Methods

Dogs

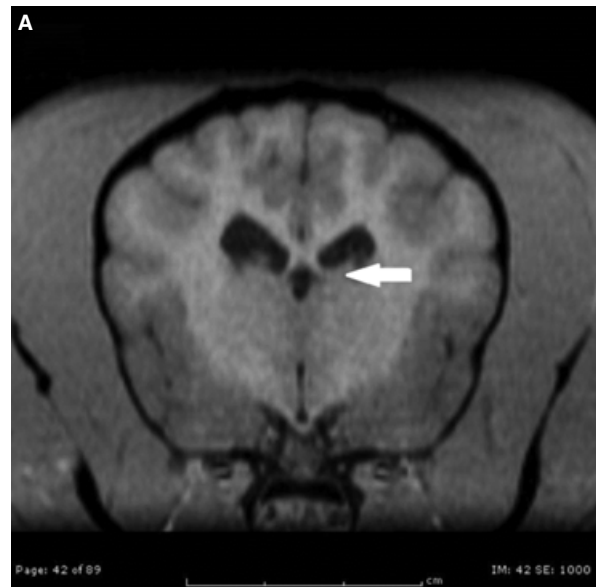
This study was performed in accordance with the guidelines of the University of Melbourne Animal Ethics Committee. Four adult male Greyhound dogs, between 1 and 4 years of age, were used for this study. The dogs ranged between 30 and 35 kg in body weight. Before the study, complete clinical and neurologic examinations and hematology and biochemistry testing were performed to ensure that the animals were healthy and neurologically normal.

Imaging

Anesthesia was performed with a standard regimen for both imaging and surgery: premedication with acepromazine^a (0.03 mg/kg SC) and buprenorphine^b (20 µg/kg SC), followed by induction with alfaxalone^c (2 mg/kg IV), intubation and maintenance using alfaxalone and fentanyl^d infusion (0.2 and 0.4 µg/kg/min IV, respectively). On the day of imaging, after induction of anesthesia, a midline skin incision 8 cm long was made over the frontal bone and a fiducial array^e was attached to the frontal bone using ceramic screws before imaging was performed with a 1.5T MRI.^f The following image sequences were acquired with the animal in a standard knee coil: sagittal and transverse plane T2-weighted images and dorsal plane T1 3D images, which then were reconstructed into transverse and sagittal plane images with 0.5-mm thickness. Image data were downloaded and transferred to a target planning system^b for target identification (Fig 1) and trajectory planning. Trajectories for unilateral thalamic DBS leads^g and hippocampal recording electrodes^h were calculated based on images and designed to avoid the ventricles and vascular structures. After imaging and trajectory planning, the baseplate of the fiducial array was left in place, the skin was sutured over the frontal bone, and the animal recovered until the day of surgery.

Surgery

On the day of surgery, animals were anesthetized as described previously and placed in sternal recumbency with the head elevated 20 cm from the operating table with the hard palate parallel to the table. The skin over the head and the neck was clipped and prepared aseptically. The fiducial array baseplate then was exposed and the Brainsight frame applied, after which registration was performed as described by other authors.²⁶ A standard rostromedial approach was performed



B

#1200

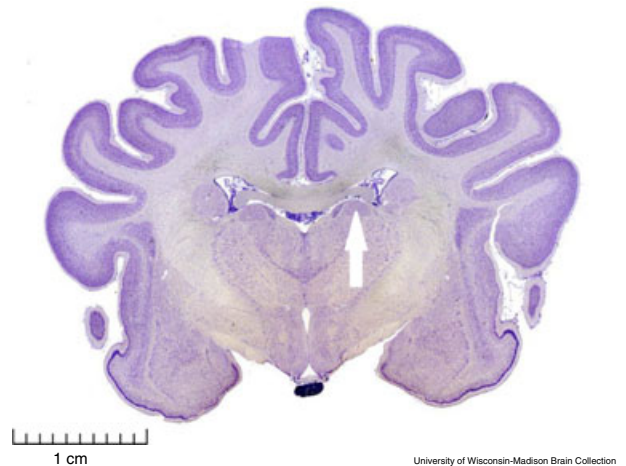


Fig 1. MRI (A) and histologic (B) transverse plane sections of the canine brain taken at the level of the thalamus. Arrows indicate the cranial nucleus of the thalamus. Image (B) reproduced from the University of Wisconsin–Madison comparative mammalian brain collection.

to expose the skull on the left side of the dog and the Brainsight system used to plan and mark the entry holes for insertion of both leads. After calculation of skull thickness, 15-mm holes were drilled in the calvarium using a guide and depth stop along the preplanned trajectory. The meninges were perforated using a dural hook and the Brainsight system was then used to calculate the depth of placement of each lead before a cannula and stylette of appropriate diameter were advanced along the trajectory to the calculated depth. The DBS lead was 0.6 mm in diameter and 12.0 cm in length with four 0.5 mm electrodes spaced 0.5 mm apart, whereas the hippocampal recording lead was 1.2 mm in diameter with four 1.5 mm electrodes spaced 0.5 mm apart. After withdrawal of the stylette, leads were advanced through the cannula to depth and the cannula then removed while the leads were held in place at the skull surface with De Baky forceps. Leads were secured to the skull using methylmethacrylate bone cement in conjunction with ceramic

screws inserted into the skull approximately 10 mm away from each burr hole.

A second incision approximately 15 cm long was made on dorsal midline over the caudal cervical spine to insert the implantable DBS pulse generator and recording device.²⁷ The device was implanted into a pocket created by blunt dissection between layers of the rhomboideus muscle on the left side of the dog 10–15 cm cranial to the cranial border of the scapula. Stimulating and recording leads were connected to extensions, which then were tunneled SC using alligator forceps from the cranial incision to the pulse generator and recording device. Before closing both sites, impedance of the electrodes in each lead was checked and 30 seconds of EEG activity was recorded from each pair of electrodes. Typical impedance for adjacent bipolar electrode pairs was approximately 1,000 Ω . Both surgical sites were closed in routine fashion with absorbable suture material.

Postoperative Imaging and Recovery

After surgery, dogs were imaged by CT scan in the transverse plane before recovery.¹ Linear transformation of CT and MRI scans was performed to align the data sets of each animal, and the CT scan was overlaid on the anatomical MRI by the Brain-sight software to verify the location of the electrodes based on presurgical targeting. The planned target location coordinates (x , y , z) and actual target location coordinates (x' , y' , z') were recorded and the placement error calculated using the following formula: placement error = $\sqrt{(x - x')^2 + (y - y')^2 + (z - z')^2}$. After CT scanning, the animals were recovered and managed postoperatively with pain relief (methadone^j 0.1–0.4 mg/kg SC q4h for the first 24 hours, lignocaine^k and ketamine^l constant rate infusion at 25–50 $\mu\text{g}/\text{kg}/\text{min}$ and 0.1–0.3 mg/kg/h IV, respectively, for the first 12–14 hours, and carprofen^m 2 mg/kg PO q12h for 5 days) and antibiotic therapy (cephalexin,ⁿ 15 mg/kg BID PO q12h for 7 days). Serial neurologic examinations were performed on each dog once daily for the first 7 days, then weekly for the next 4 weeks.

Stimulation and Recording

At 7 days after surgery, the stimulating device was tested. Impedance between each pair of electrodes within both the stimulating and recording leads was checked to ensure system integrity. Test stimulations from each pair of electrodes in the thalamic DBS lead together with recording from each pair of electrodes in the hippocampal recording lead were used to establish the pair of electrodes in each lead that gave the best evoked response. Once this was established, electrical stimulation was used to identify the evoked response. Electrical stimulation was performed for 7 days before dogs were treated with levetiracetam^o at 20 mg/kg PO q8h for a total of 7 days, followed by 40 mg/kg PO q8h for 7 days (low and high dosage). The electrical stimulation consisted of biphasic pulses delivered at a rate of 2 Hz. The stimulation rate was sufficiently low to allow the transient activity from each stimulus to decay before the arrival of the subsequent stimulus. The stimulator was set in constant voltage mode with an amplitude of 3 V and a pulse width of 300 μs . Evoked potentials (EPs) were recorded with a sampling rate of 422 Hz in 33-second windows, starting every 15 minutes over the duration of the testing period. This allowed 66 electrical-evoked potentials to be recorded over the 33-second window. These parameters allowed for a sufficient number of trials for averaging within a reasonable time resolution to track excitability changes while allowing for a full day of data to be stored. The stimulator was programmed and data were downloaded by means of a hand-held communicator placed on the skin of the neck directly over the device.

Data Analysis

Data analysis consisted of 2 steps. The first involved computing the averaged EP for each of the 33 s windows, whereas the second involved extracting scalar features of the averaged EPs that were descriptive of their shape. The average EPs were computed by aligning each individual EP using the stimulation artifacts. The artifacts were extracted from the signals by first up-sampling the data by a factor of 4, then computing the forward difference of the recorded time series before applying a threshold of 4 standard deviations from the mean. The time of the first sample to cross this threshold for each stimulus was used to segment the stimuli. The EPs were extracted with a window of 20 ms before and 200 ms after each stimulation artifact detection. The features of the averaged EPs considered were the amplitude of the largest peak, and the time to reach the peak relative to the stimuli. These were chosen because they were likely to vary with changes in excitability within the network, as well as for computational simplicity. Only the latency of the dominant peak relative to the stimulus is presented in the results section.

Results

Lead Placement

No complications were encountered during placement of the cannulas and stylettes, which was performed slowly but firmly with a clockwise rotating movement to aid cannula insertion. In 1 dog (dog number 2), CSF was encountered after the stylette was withdrawn during placement of the ANT electrode, suggesting that the left lateral ventricle had been entered during cannula placement. Because of the small size of the Numed lead, caution was taken to avoid accidentally moving or completely withdrawing the lead with the cannula. In addition, kinking or bending the lead excessively would have resulted in substantial damage, necessitating gentle handling during the procedure. Grasping the lead lightly with DeBakey forceps to hold the lead in place while withdrawing the cannula was found to be the most reliable means of maintaining the lead's position before fixation.

In 3 of the 4 dogs, postsurgery CT scans and coregistration with preoperative MRI confirmed that all leads had electrodes located within both the ANT and the hippocampus. Figures 2 and 3 show coregistered postoperative CT and preoperative MRI scans. In dog 1, the tip of the ANT lead was noted to be medial to the planned target and the distal part of the lead was located within the lateral ventricle, although no CSF was encountered during lead placement. The tip of the hippocampal electrode was noted to be distal to the planned target in the entorhinal cortex, with all other contacts within the hippocampus. In dog 2, the tip of the ANT lead was found to have crossed midline, but the proximal electrodes were correctly located within the anterior nucleus. The hippocampal lead was very well positioned, with the most proximal electrode within the parahippocampus. However, the presence of CSF intraoperatively suggested that the canula entered the lateral ventricle on the way to the target. In dog 3, both leads were found to be located outside

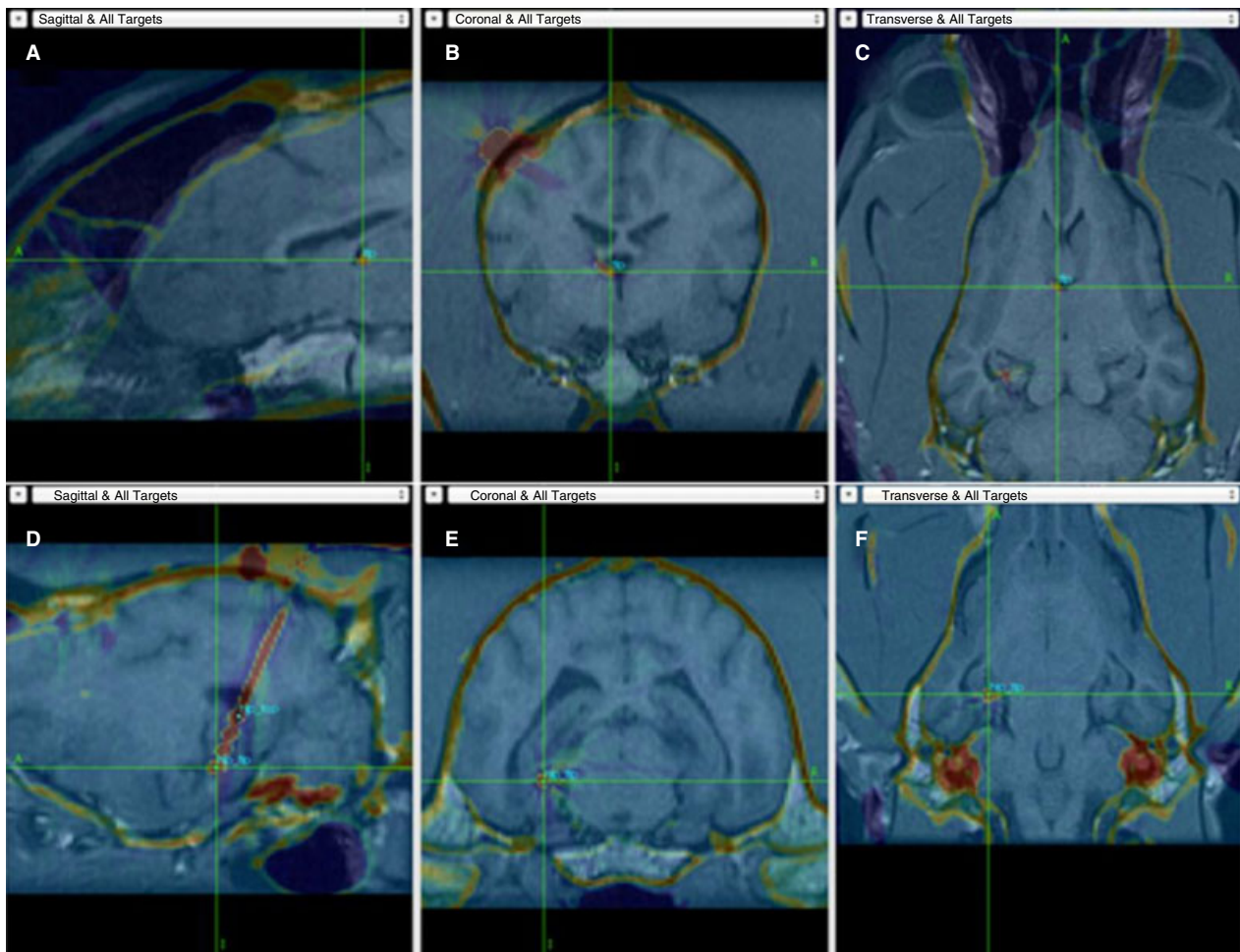


Fig 2. Merged MRI and postoperative CT images of dog 4 in sagittal (A, D), transverse (B, E), and dorsal (C, F) planes. The electrodes are shown in red with the green crosshairs identifying the distal end of the ANT electrode (A, B, C) and hippocampal electrode (D, E, F).

of the calvarium. However, tracts visible within the brain together with impedance measurements and EEG recording intraoperatively suggested that initial placement of the leads was correct, and that the leads were dislodged during closure after implantation. In dog 4, both the ANT and the hippocampal leads were found to be perfectly positioned in the anterior nucleus and hippocampus, respectively, although again the most proximal hippocampal lead electrode was found to be located within the parahippocampus. In the 3 dogs with successful electrode placement, the placement error between the intended target and final location of the tip of each lead is shown in Table 1. Overall, for those dogs in which leads were correctly placed, the mean lead placement error (with 95% confidence interval) for all target sites was 4.60 ± 1.5 mm.

Postoperative Recovery

In 3 of 4 dogs, recovery was routine with no clinically relevant abnormalities. In 1 dog, excessive movement during the recovery period resulted in the

formation of a large subcutaneous hematoma on the dorsal midline over the stimulation device. This was managed conservatively with a combination of wet-dry dressings and placement of a Penrose drain and resolved over the next week. In all dogs, postoperative pain associated with the craniotomy required a mixture of opioid medication and lignocaine and ketamine constant rate infusions to adequately control discomfort, similar to routine postoperative analgesia for craniotomies at our institution. Clinical and neurologic examinations performed in the postoperative period identified no clinically relevant abnormalities in any dog. Recovery from surgery was complete in all dogs within 24 hours after surgery, although some discomfort was noted for up to 5 days after surgery, which was treated with carprofen as described. Serial neurologic examinations over the next 4 weeks showed no other abnormalities in any of the dogs.

Stimulation and Recording

Evoked Responses. Figure 4 shows 10-second recordings of EEG activity with and without stimulus

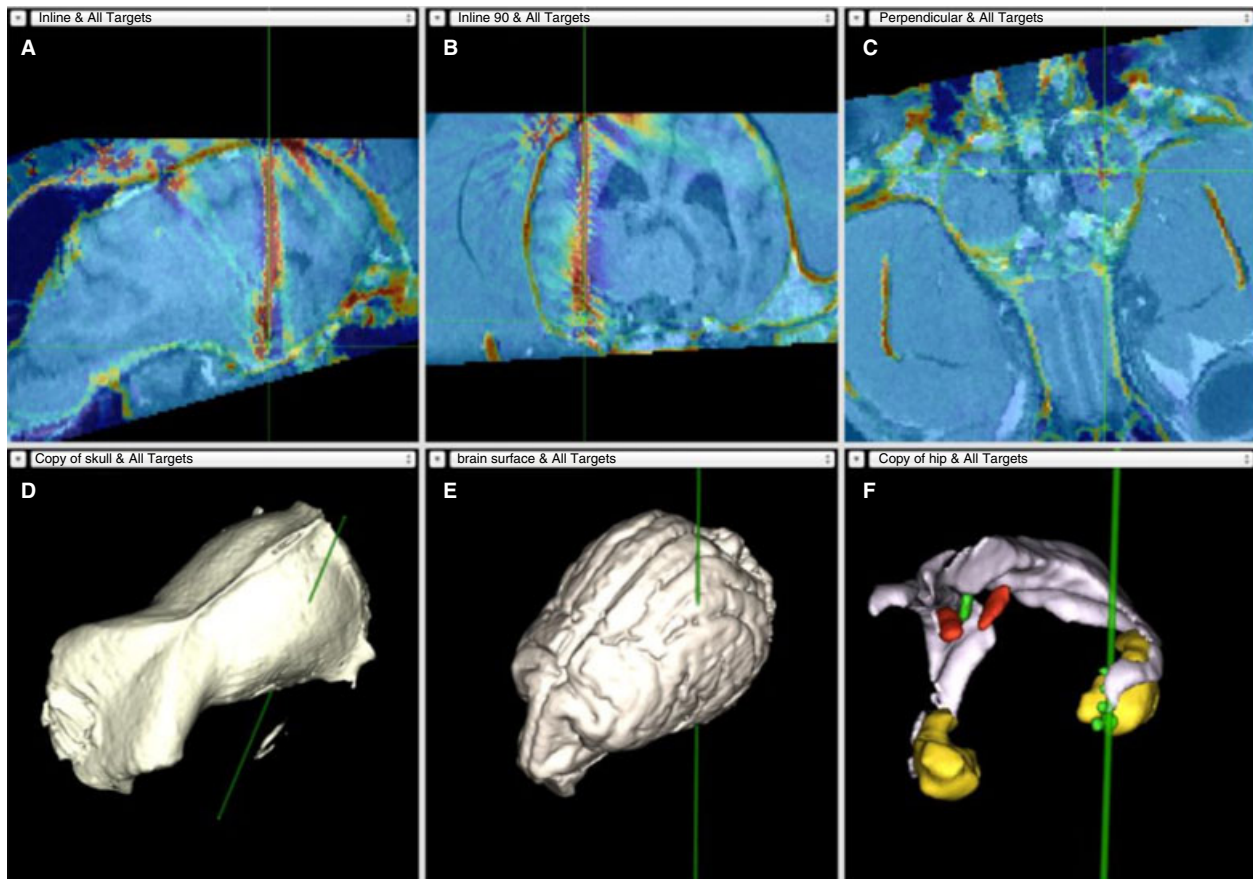


Fig 3. Merged MRI and postoperative CT images taken from dog 2 (A, B, C) together with illustrations of hippocampal electrode trajectory (green line) during placement relative to reconstructions of skull (D), brain (E), and hippocampus and ANT (yellow and red, respectively) (F). Electrode contacts are shown as green, with the ventricles shown in gray in (F).

Table 1. Placement error for ANT and hippocampal electrodes.

Dog Number	ANT Electrode Placement Error (mm)	Hippocampal Electrode Placement Error (mm)
1	4.04	6.49
2	6.01	2.19
4	4.06	4.83
All dogs		
Mean error all electrodes		4.60
SD		1.55

applied. Figure 5 shows the morphology of the averaged EPs over the experimental period together with variation in the time-to-peak amplitude on consecutive days. Averaged EPs displayed a wave with latency of approximately 40 ms and amplitude of 0.02 mV, consistent with activation of the Circuit of Papez as seen in sheep models.²² Interestingly, there was a slight decrease in EP amplitude that occurred approximately 1 hour after each dose of levetiracetam once this was initiated (Fig 5).

Discussion

This study showed that it is feasible to place DBS and recording electrodes in the thalamus and hippocampus of dogs with accuracy and with minimal morbidity. Using the Brainsight system, an overall mean accuracy of 4.6-mm placement error was achieved in the dogs with successful fixation. Given the size and spacing of the electrodes, this accuracy allowed the positioning of at least 1 electrode in the target in all dogs. In all cases, the dogs recovered without adverse neurologic effects and showed no outward sign of the effects of the implantation or stimulation. In addition, stimulation and recording from the electrodes showed that stimulation of the ANT can produce evoked responses identical to those obtained in other large animal models in which similar studies have been performed.²² The shape and latency of the EPs was consistent with activation of the circuit of Papez, suggesting that the dog is a suitable model for the testing of DBS strategies in the treatment of epilepsy.

To the authors' knowledge, this is the first report to describe the implantation of indwelling electrodes in the brain of dogs for the purposes of recording and stimulating simultaneously. Other studies in the field

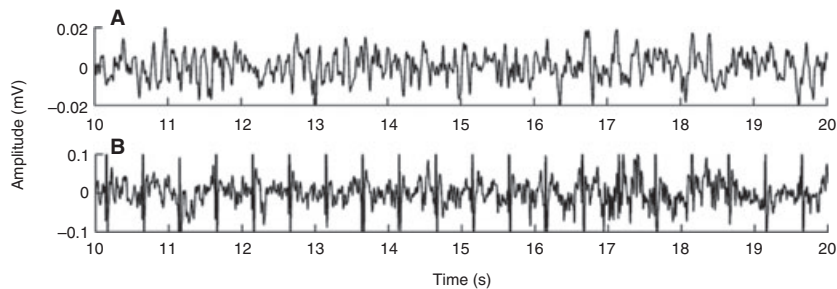


Fig 4. EEG recordings taken before (A) and after (B) initiation of stimulations from the hippocampus of dog 1. Each strip represents 10 seconds of recording.

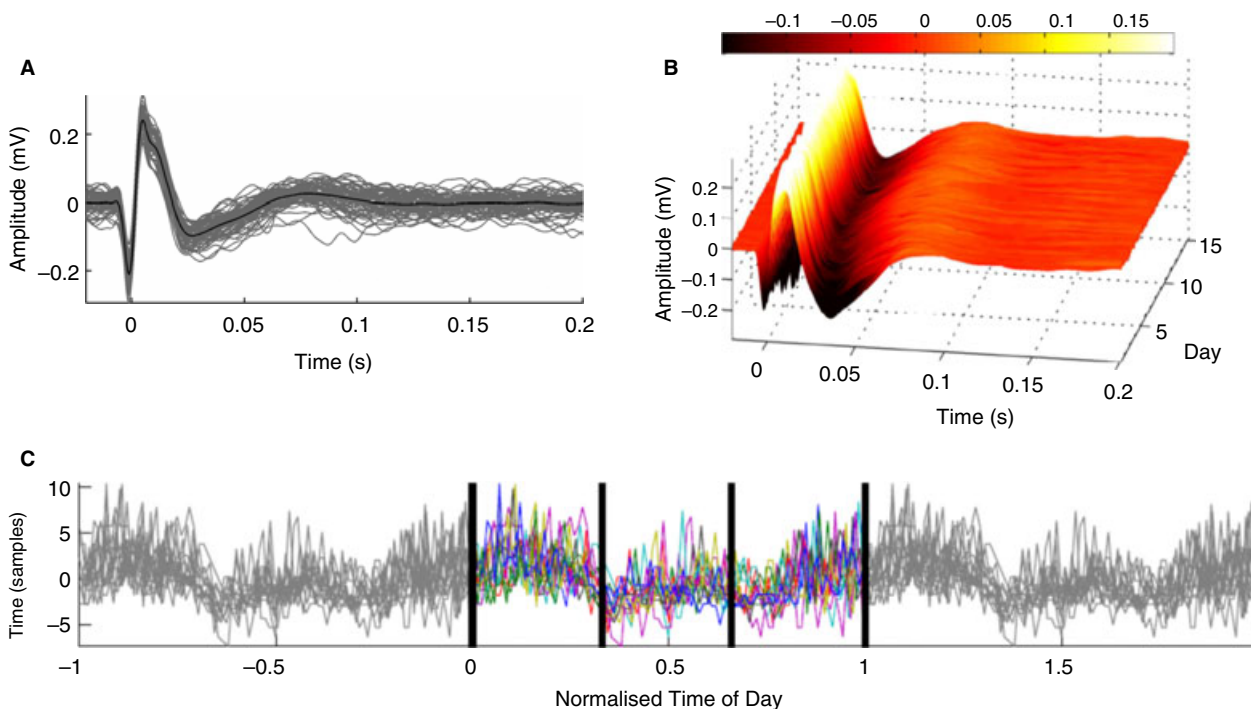


Fig 5. Averaged evoked potentials (EPs) after stimulation. (A) shows an average of 66 33-second recordings, with (B) showing a montage of EPs from the hippocampus of dog 4 over a period of 14 days. (C) shows the influence of levetiracetam on the time-to-peak amplitude of the EPs recorded from dog 4. The colored lines represent the overlay of all days on treatment, with black bars representing the time at which each dose was given and arrows indicating the decrease in time-to-peak amplitude associated with each dose.

of veterinary medicine have examined the use of stereotaxy for needle placement, but predominantly in the setting of lesion biopsy.^{28–31} In addition, studies have examined image-guided freehand or directed biopsy techniques, both to biopsy lesions³² and to implant indwelling catheters for delivering brachytherapy.²⁵ Overall, the morbidity and mortality described in most studies in dogs is low, ranging from 12 to 29% and 6 to 9%, respectively.^{28,30,32} This is higher than the 3–12% morbidity rate and 0–1% mortality rate reported in human patients.^{33,34} The limited numbers in our study do not allow for direct comparison, but the use of the Brainsight system to implant electrodes did not result in any neurologic deficits in any of the dogs involved. It is likely that the implantation

of these electrodes is a safer procedure because there is no suction applied to the brain parenchyma and therefore the risk of intracranial hemorrhage is smaller than with needle biopsy. In addition, the dogs in this study had no structural pathology, as compared with dogs undergoing needle biopsy to diagnose lesions, in which the presence of additional blood vessels within the lesions would increase the likelihood of hemorrhage, the biggest cause of postbiopsy morbidity.

Given the small size of some of the targets involved, such as the ANT, obtaining accurate electrode placement is extremely important in a trial such as the one reported here. A mean placement error of 4.6 mm was acceptable, given that in all cases, this allowed for contact of at least 1 pair of contacts with

the target, although further testing in more cases is necessary to definitively assess accuracy of placement. Several factors are likely to have contributed to the placement error. When using the Brainsight system, a registration to the animal's MRI scans is obtained by locating homologous markers on the animal and on the display using an optical position sensor. In people, frameless stereotaxy devices, such as the Brainlab and Stealth systems, use up to 9 registration points glued to the skin over the skull, as compared with the 5 registration points clustered around the front of the skull with the Brainsight system.^{35,36} The difficulties associated with gluing and maintaining registration points to the skin and the mobility of the skin in dogs precludes this possibility. As a result, the registration process involves some error, and the further away the subsequent trajectory is from the registration device located on the frontal bone, the more this error is exaggerated. Differences in skull shape and size among breeds are also likely to contribute to challenges in lead placement, because a smaller skull results in a greater distance between the frame and the target. In addition, the smaller brachycephalic skull shape offers less scope for an accurate lateral approach for lead placement. Finally, it is likely that movement of the electrodes occurred during or after stylette placement, which in some cases was >5 mm. Solutions to improve this currently are being examined, and in the future, different methods of maintaining the electrodes in place and of securing them to the calvarium will be utilized. In humans, special securing devices such as the Guardian burr hole cap are available that are placed in the burr hole and which then have a locking cap overlaid to secure the lead. It is likely that future improvements will involve

a similar solution. Finally, the process of fusing the CT scans and MRI scans is imperfect and the hyperdense appearance of the electrode tips on CT scan makes the precise location of the electrode tip difficult to determine. Some studies have utilized the superior soft tissue imaging characteristics of MRI to image DBS electrodes during or after placement to establish the exact location of contact points.^{37–39} However, the presence of ferromagnetic material in the electrodes raises the concern of thermal injuries when MRI is performed, as well as generating a signal void as a result of local distortion of the magnetic field.³⁹ For these reasons, CT generally is regarded as a safer modality for postoperative imaging. The exaggerated appearance of the electrodes on CT has been characterized, with a 1.27-mm lead having been shown to generate an artifact of up to 3.4 mm.³⁹ For this reason, fusing postoperative CT images with preoperative MRI is commonly used to combine the anatomical accuracy of MRI images with the safety of CT, and studies have shown the registration of the 2 involves a discrepancy of approximately 1.5 mm.³⁹ Therefore, a substantial proportion of the placement error in this study is likely to have been arisen from the fusion of CT and MRI images. In the future, the use of improved electrodes may allow MRI scanning to replace CT scanning as the modality of choice for postoperative assessment. This would eliminate the error associated with fusion of the 2 images while simultaneously evaluating small amounts of hemorrhage or edema associated with the procedure.

The rationale for stimulation of the ANT as part of seizure therapy comes from the discovery that the ANT plays a crucial role in the propagation of limbic epilepsy as part of the Papez circuit (Fig 6). The

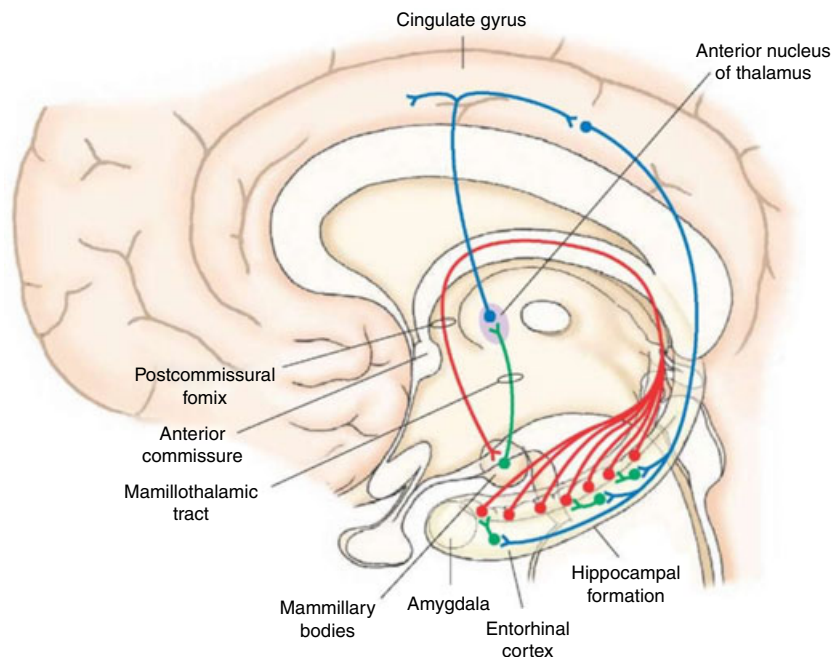


Fig 6. The Circuit of Papez. Reproduced from <http://what-when-how.com/neuroscience>.

Papez circuit was described in 1937 by James Papez as a circuit linking hippocampal output via the fornix and mammillary nucleus in the posterior hypothalamus to the ANT.⁴⁰ The ANT projects to the cingulum bundle deep to the cingulate gyrus, which travels around the wall of the lateral ventricle to the parahippocampal cortex. This structure then completes the circuit by returning to the hippocampus. Atrophy or sclerosis of any structures within the circuit has been known to cause epilepsy, as occurs with mesial temporal sclerosis.⁴¹ Although mesial temporal sclerosis has yet to be described in dogs, the importance of the Papez circuit in the propagation of seizure activity suggests that it remains an important target for the treatment of epilepsy in dogs. Two other circuits are believed to be involved in the propagation of seizures: the corticothalamic circuit and the mammillary circuit. The corticothalamic circuit involves propagation of seizure activity from the motor cortex to the caudate, putamen, the globus pallidus and the thalamus,⁸ and unilateral, repeated stimulation of this circuit can result in continual partial seizures.⁴² The mammillary circuit also involves the ANT, from which seizure activity is propagated to the mammillary bodies to the brainstem.⁸

Targeting of these circuits in the treatment of epilepsy is based on the theory that stimulation delivered to these pathways can prevent the generalization and propagation of seizures,⁴³ although the exact mechanisms remain unclear.⁴⁴ It is known that the unilateral stimulation of the anterior thalamus in amygdala-kindled seizures in rats decreases the incidence of generalized seizures.⁴⁵ EEG and concurrent thalamic recording after surgery in human patients are consistent with a recruitment pattern that correlates with clinical improvement.⁴⁶ Several studies of ANT stimulation have been performed, the largest of which is a multicenter, double-blind, randomized clinical trial entitled Stimulation of the Anterior Nucleus of the Thalamus for Epilepsy (SANTE).⁹ The treatment group of the 110 patients in the SANTE trial showed a median seizure frequency reduction of 29% at 3 months, 41% at 1 year, 56% at 2 years, and 68% by the end of 3 years as compared with baseline. Other, smaller, nonrandomized trials of ANT stimulation also have been performed with 4–6 patients per trial, with seizure frequency reduction of 14–75%.^{9,11,16–19}

Perhaps the most exciting prospect raised by this trial is the possibility of closed loop recording and stimulation for the treatment of epilepsy. Long-term stimulation has been performed in human patients for a number of years, and long-term EEG recording recently has become available, but the device described here is one of the first that combines both capabilities simultaneously. This, in turn, raises the prospect of intelligent stimulation that can be instigated in response to seizure activity as detected in the EEG recording. Such devices would represent an important advance in brain stimulation for the treatment of epilepsy, and potentially could revolutionize the lives of human and canine patients with epilepsy.

Footnotes

- ^a ACP2, Delvet P/L, Seven Hills, Australia
^b Temgesic, Reckitt Benckiser, West Ryde, Australia
^c Alfaxan, Jurox P/L, Rutherford, Australia
^d DBL Fentanyl Injection, Hospira Australia P/L, Melbourne, Australia
^e Brainsight, Rogue Research Inc, Montreal, Canada
^f Signa, GE Healthcare, Buckinghamshire, UK
^g NuMED primate electrode, NuMed Inc, Hopkinton, MA
^h DBS lead model 3387, Medtronic Inc, Minneapolis, MN
ⁱ Somatom Emotion 16, Siemens Medical Solutions P/L, Bayswater, Australia
^j Physeptone, Sigma Pharmaceuticals, Croydon, Australia
^k Lignocaine, Troy Laboratories P/L, Glendenning, Australia
^l Ketamine, Parnell Australia P/L, Alexandria, Australia
^m Rimadyl, Pfizer Australia P/L, West Ryde, Australia
ⁿ Cephalixin, Apex Laboratories P/L, Somersby, Australia
^o Keppra, UCB Pharma, Malvern, Australia
-

Acknowledgment

This work was performed at the University of Melbourne Veterinary Hospital.

This study was supported by a grant from Medtronic Inc.

Conflict of Interest: Authors disclose no conflict of interest.

References

- Zimmermann R, Hulsmeier V, Sauter-Louis C, et al. Status epilepticus and epileptic seizures in dogs. *J Vet Intern Med* 2009;23:970–976.
- Saito M, Munana KR, Sharp NJ, et al. Risk factors for development of status epilepticus in dogs with idiopathic epilepsy and effects of status epilepticus on outcome and survival time: 32 cases (1990–1996). *J Am Vet Med Assoc* 2001;219:618–623.
- Chang Y, Mellor DJ, Anderson TJ. Idiopathic epilepsy in dogs: Owners' perspectives on management with phenobarbitone and/or potassium bromide. *J Small Anim Pract* 2006;47:574–581.
- Berendt M, Gredal H, Ersboll AK, et al. Premature death, risk factors, and life patterns in dogs with epilepsy. *J Vet Intern Med* 2007;21:754–759.
- Cunningham JG, Farnbach GC. Inheritance and idiopathic canine epilepsy. *J Am Anim Hosp Assoc* 1988;24:421–424.
- Milne ME, Anderson GA, Chow KE, et al. Description of technique and lower reference limit for magnetic resonance imaging of hippocampal volumetry in dogs. *Am J Vet Res* 2013;74:224–231.
- Sander JW. Some aspects of prognosis in the epilepsies: A review. *Epilepsia* 1993;34:1007–1016.
- Zhong XL, Yu JT, Zhang Q, et al. Deep brain stimulation for epilepsy in clinical practice and in animal models. *Brain Res Bull* 2011;85:81–88.
- Fisher R, Salanova V, Witt T, et al. Electrical stimulation of the anterior nucleus of thalamus for treatment of refractory epilepsy. *Epilepsia* 2010;51:899–908.
- Morrell MJ. Group RNSiES. Responsive cortical stimulation for the treatment of medically intractable partial epilepsy. *Neurology* 2011;77:1295–1304.

11. Andrade DM, Zumsteg D, Hamani C, et al. Long-term follow-up of patients with thalamic deep brain stimulation for epilepsy. *Neurology* 2006;66:1571–1573.
12. Chabardes S, Kahane P, Minotti L, et al. Deep brain stimulation in epilepsy with particular reference to the subthalamic nucleus. *Epileptic Disord* 2002;4(Suppl 3):S83–S93.
13. Chkhenkeli SA, Sramka M, Lortkipanidze GS, et al. Electrophysiological effects and clinical results of direct brain stimulation for intractable epilepsy. *Clin Neurol Neurosurg* 2004;106:318–329.
14. Fisher RS, Uematsu S, Krauss GL, et al. Placebo-controlled pilot study of centromedian thalamic stimulation in treatment of intractable seizures. *Epilepsia* 1992;33:841–851.
15. Handforth A, DeSalles AA, Krahl SE. Deep brain stimulation of the subthalamic nucleus as adjunct treatment for refractory epilepsy. *Epilepsia* 2006;47:1239–1241.
16. Hodaie M, Wennberg RA, Dostrovsky JO, et al. Chronic anterior thalamus stimulation for intractable epilepsy. *Epilepsia* 2002;43:603–608.
17. Kerrigan JF, Litt B, Fisher RS, et al. Electrical stimulation of the anterior nucleus of the thalamus for the treatment of intractable epilepsy. *Epilepsia* 2004;45:346–354.
18. Lim SN, Lee ST, Tsai YT, et al. Electrical stimulation of the anterior nucleus of the thalamus for intractable epilepsy: A long-term follow-up study. *Epilepsia* 2007;48:342–347.
19. Osorio I, Overman J, Giftakis J, et al. High frequency thalamic stimulation for inoperable mesial temporal epilepsy. *Epilepsia* 2007;48:1561–1571.
20. Velasco AL, Velasco F, Jimenez F, et al. Neuromodulation of the centromedian thalamic nuclei in the treatment of generalized seizures and the improvement of the quality of life in patients with Lennox-Gastaut syndrome. *Epilepsia* 2006;47:1203–1212.
21. Nagel SJ, Najm IM. Deep brain stimulation for epilepsy. *Neuromodulation* 2009;12:270–280.
22. Stypulkowski PH, Giftakis JE, Billstrom TM. Development of a large animal model for investigation of deep brain stimulation for epilepsy. *Stereotact Funct Neurosurg* 2011;89:111–122.
23. Stypulkowski PH, Stanslaski SR, Denison TJ, et al. Chronic evaluation of a clinical system for deep brain stimulation and recording of neural network activity. *Stereotact Funct Neurosurg* 2013;91:220–232.
24. Munana KR, Vitek SM, Tarver WB, et al. Use of vagal nerve stimulation as a treatment for refractory epilepsy in dogs. *J Am Vet Med Assoc* 2002;221:977–983.
25. Packer RA, Freeman LJ, Miller MA, et al. Evaluation of minimally invasive excisional brain biopsy and intracranial brachytherapy catheter placement in dogs. *Am J Vet Res* 2011;72:109–121.
26. Chen AV, Wininger FA, Frey S, et al. Description and validation of a magnetic resonance imaging-guided stereotactic brain biopsy device in the dog. *Vet Radiol Ultrasound* 2012;53:150–156.
27. Stanslaski S, Cong P, Carlson D, et al. An implantable bi-directional brain-machine interface system for chronic neuroprosthesis research. *Conference Proc IEEE Eng Med Biol Soc* 2009;2009:5494–5497.
28. Koblik PD, LeCouteur RA, Higgins RJ, et al. CT-guided brain biopsy using a modified Pelorus Mark III stereotactic system: Experience with 50 dogs. *Vet Radiol Ultrasound* 1999;40:434–440.
29. Koblik PD, LeCouteur RA, Higgins RJ, et al. Modification and application of a Pelorus Mark III stereotactic system for CT-guided brain biopsy in 50 dogs. *Vet Radiol Ultrasound* 1999;40:424–433.
30. Moissonnier P, Blot S, Devauchelle P, et al. Stereotactic CT-guided brain biopsy in the dog. *J Small Anim Pract* 2002;43:115–123.
31. Troxel MT, Vite CH. CT-guided stereotactic brain biopsy using the Kopf stereotactic system. *Vet Radiol Ultrasound* 2008;49:438–443.
32. Flegel T, Oevermann A, Oechtering G, et al. Diagnostic yield and adverse effects of MRI-guided free-hand brain biopsies through a mini-burr hole in dogs with encephalitis. *J Vet Inter Med* 2012;26:969–976.
33. Gempt J, Buchmann N, Ryang YM, et al. Frameless image-guided stereotaxy with real-time visual feedback for brain biopsy. *Acta Neurochir* 2012;154:1663–1667.
34. Woodworth GF, McGirt MJ, Samdani A, et al. Frameless image-guided stereotactic brain biopsy procedure: Diagnostic yield, surgical morbidity, and comparison with the frame-based technique. *J Neurosurg* 2006;104:233–237.
35. Gumprecht HK, Widenka DC, Lumenta CB. BrainLab VectorVision Neuronavigation System: Technology and clinical experiences in 131 cases. *Neurosurgery* 1999;44:97–104; discussion 104–105.
36. Barazi SA, Cudlip S, Marsh H. Awake craniotomy using stealth frameless stereotaxy without rigid skull fixation. *Br J Neurosurg* 2006;20:43–45.
37. Papavassiliou E, Rau G, Heath S, et al. Thalamic deep brain stimulation for essential tremor: Relation of lead location to outcome. *Neurosurgery* 2008;62(Suppl 2):884–894.
38. Saint-Cyr JA, Hoque T, Pereira LC, et al. Localization of clinically effective stimulating electrodes in the human subthalamic nucleus on magnetic resonance imaging. *J Neurosurg* 2002;97:1152–1166.
39. Thani NB, Bala A, Swann GB, et al. Accuracy of postoperative computed tomography and magnetic resonance image fusion for assessing deep brain stimulation electrodes. *Neurosurgery* 2011;69:207–214; discussion 214.
40. Carpenter MB. *Core Text of Neuroanatomy*, 4th ed. Baltimore, MD: Williams and Wilkins; 1991.
41. Oikawa H, Sasaki M, Tamakawa Y, et al. The circuit of Papez in mesial temporal sclerosis: MRI. *Neuroradiology* 2001;43:205–210.
42. Takebayashi S, Hashizume K, Tanaka T, et al. The effect of electrical stimulation and lesioning of the anterior thalamic nucleus on kainic acid-induced focal cortical seizure status in rats. *Epilepsia* 2007;48:348–358.
43. Lega BC, Halpern CH, Jaggi JL, et al. Deep brain stimulation in the treatment of refractory epilepsy: Update on current data and future directions. *Neurobiol Disease* 2010;38:354–360.
44. Pereira EA, Green AL, Stacey RJ, et al. Refractory epilepsy and deep brain stimulation. *J Clin Neurosci* 2012;19:27–33.
45. Zumsteg D, Lozano AM, Wennberg RA. Rhythmic cortical EEG synchronization with low frequency stimulation of the anterior and medial thalamus for epilepsy. *Clin Neurophysiol* 2006;117:2272–2278.
46. Lado FA. Chronic bilateral stimulation of the anterior thalamus of kainate-treated rats increases seizure frequency. *Epilepsia* 2006;47:27–32.